Bioorganic & Medicinal Chemistry Letters 21 (2011) 3307–3312

Contents lists available at ScienceDirect

Bioorganic & Medicinal Chemistry Letters

journal homepage: www.elsevier.com/locate/bmcl

Phosphodiesterase inhibitors. Part 1: Synthesis and structure–activity relationships of pyrazolopyridine–pyridazinone PDE inhibitors developed from ibudilast

Robert W. Allcock [a], Haakon Blakli [a], Zhong Jiang [a], Karen A. Johnston [a], Keith M. Morgan [a], Georgina M. Rosair [a], Kazuhiko Iwase [b], Yasushi Kohno [b], David R. Adams [a,*]

[a] Chemistry Department, School of Engineering and Physical Sciences, Heriot-Watt University, Riccarton, Edinburgh EH14 4AS, United Kingdom
[b] Discovery Research Laboratories, Kyorin Pharmaceutical Co., Ltd, 2399-1, Nogi, Nogi-machi, Shimotsuga-gun, Tochigi 329-0114, Japan

ARTICLE INFO

Article history:
Received 21 February 2011
Revised 2 April 2011
Accepted 6 April 2011
Available online 13 April 2011

Keywords:
Cyclic 3′,5′-nucleotide phosphodiesterase (PDE)
Ibudilast
PDE3 inhibitors
PDE4 inhibitors
Respiratory disease

ABSTRACT

Ibudilast [1-(2-isopropylpyrazolo[1,5-*a*]pyridin-3-yl)-2-methylpropan-1-one] is a nonselective phosphodiesterase inhibitor used clinically to treat asthma. Efforts to selectively develop the PDE3- and PDE4-inhibitory activity of ibudilast led to replacement of the isopropyl ketone by a pyridazinone heterocycle. Structure–activity relationship exploration in the resulting 6-(pyrazolo[1,5-*a*]pyridin-3-yl)pyridazin-3(2*H*)-ones revealed that the pyridazinone lactam functionality is a critical determinant for PDE3-inhibitory activity, with the nitrogen preferably unsubstituted. PDE4 inhibition is strongly promoted by introduction of a hydrophobic substituent at the pyridazinone N(2) centre and a methoxy group at C-7′ in the pyrazolopyridine. Migration of the pyridazinone ring connection from the pyrazolopyridine 3′-centre to C-4′ strongly enhances PDE4 inhibition. These studies establish a basis for development of potent PDE4-selective and dual PDE3/4-selective inhibitors derived from ibudilast.

The cyclic 3′,5′-nucleotide phosphodiesterases (PDEs) play pivotal roles in shaping spatial and temporal gradients of the signalling second messengers, cAMP and cGMP, mediating their hydrolysis to 5′-AMP and 5′-GMP, respectively. There are 11 PDE gene families, with enzymes belonging to the PDE3, PDE4 and PDE5 families having received greatest attention to date as targets for chemotherapeutic interventions. Inhibitors of cGMP-specific PDE5 have been successfully deployed in the treatment of male erectile dysfunction and pulmonary arterial hypertension.[1] Isoforms of the PDE3 and PDE4 families regulate cAMP levels, with the PDE3 inhibitor, milrinone (Fig. 1), used clinically for acute management of cardiogenic shock that is unresponsive to alternative treatments.[2] Development of PDE3 inhibitors was largely curtailed in the 1990s when clinical data emerged that linked their long-term application in heart failure patients to reduced survival rates.[3] Despite these adverse data, recent years have seen a resurgence of interest in PDE3 as a target allied to efforts to develop isoform-selective PDE inhibitors with improved pharmacological profiles.[4] Efforts to harness the therapeutic potential of PDE4 inhibitors have been substantially focused on anti-inflammatory applications in asthma, chronic obstructive pulmonary disease (COPD), atopic dermatitis and rheumatoid arthritis,[5] but the cognitive enhancing properties of PDE4 inhibitors have also received attention.[5c,6] Roflumilast (Fig. 1) recently became the first PDE4-selective inhibitor to gain regulatory approval (for use within the European Union) and is indicated for severe COPD.[7] The anti-inflammatory activity of PDE4 inhibitors as a potential treatment for asthma is augmented by additional, if modest, bronchodilatory activity.[8] PDE3 inhibitors are reportedly[9] superior to PDE4 inhibitors in mediating airways smooth muscle relaxation, however, leading some groups to explore the therapeutic potential of dual PDE3/4 inhibitors.[10]

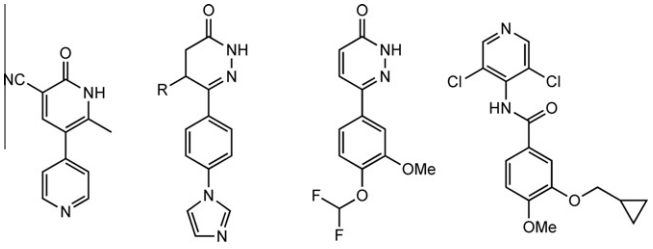

Figure 1. Structures of selected PDE3- and PDE4-inhibitors.

* Corresponding author.
E-mail address: D.R.Adams@hw.ac.uk (D.R. Adams).

0960-894X/$ - see front matter © 2011 Elsevier Ltd. All rights reserved.
doi:10.1016/j.bmcl.2011.04.021

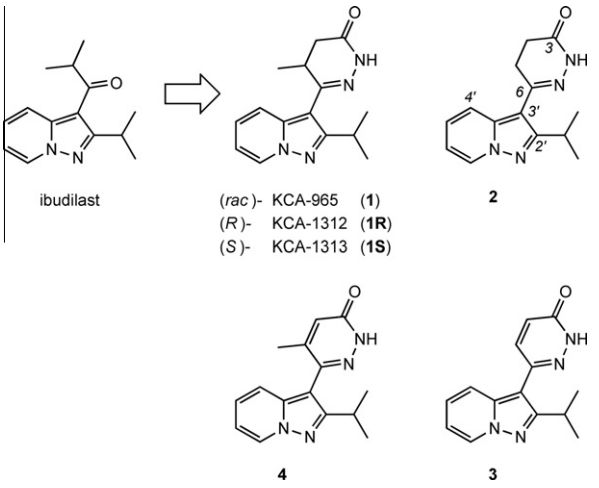

Figure 2. Ibudilast and prototypical compounds of a new PDE-inhibitory series of 6-(pyrazolo[1,5-*a*]pyridin-3-yl)pyridazin-3(2*H*)-ones.

Ibudilast (Fig. 2) is a nonselective PDE inhibitor used in Japan to treat allergies and asthma. The compound inhibits PDE3, PDE4 and PDE5 isoforms with K_i values ranging from 3.3 to 78 μM, but it also inhibits most other PDE families in the micromolar range.[11] Efforts to selectively develop the PDE4- or dual PDE3/4-inhibitory activity of ibudilast, as part of an ongoing respiratory disease programme, led to replacement of the isopropyl ketone by the pyridazinone subunit of KCA-965 (**1**, Fig. 2).[12] Introduction of the pyridazinone was prompted by the observation that this heterocycle features in a number of PDE3 inhibitors, such as imazodan[13] and CI-930,[14] as well as the dual PDE3/4 inhibitor, zardaverine[15] (Fig. 1). Synthesis of the prototypical pyrazolopyridine–pyridazinone, KCA-965, and its enantiomers (KCA-1312, KCA-1313) has been reported previously.[12] We have also recently described the development of concise synthetic routes for the construction of a series of 6-(pyrazolo[1,5-*a*]pyridin-3-yl)pyridazin-3(2*H*)-ones related to KCA-965.[16] This synthetic programme facilitated a detailed structure–activity relationship survey for the compound series, and we summarise here the most important findings of that survey in relation to in vitro PDE3-, PDE4- and PDE5-inhibitory activity (assayed using the core catalytic domains from the PDE3A, PDE4B and PDE5A isoforms using previously reported protocols[11b]). The results of this survey provide a basis for development of potent PDE4-selective and dual PDE3/4-selective inhibitors derived from ibudilast.

The unsubstituted parent dihydropyridazinone and pyridazinone core structures **2** and **3** (Fig. 2) exhibited only modest levels of PDE-inhibitory activity (Table 1). Introduction of the 5-methyl group in KCA-965 (**1**) led to a slight enhancement in activity. Interestingly, whereas both 5-methyldihydropyridazinone enantiomers (**1R** and **1S**) exhibited comparable activity against PDE4, the (*S*)-enantiomer was essentially inactive against PDE3 and PDE5. A second striking observation was that introduction of the 5-methyl group in pyridazinone **3**, affording **4**, severely compromised activity against all three PDEs (Table 1). This loss of activity caused by methyl substitution at the sp^2-hybridised 5-position in **4** suggested a probable requirement for a near coplanar ring arrangement in the inhibitor's enzyme-bound conformation with each enzyme, and the presence of the in-plane 5-methyl group would incur a significant energy penalty for adoption of such a conformation. These considerations pointed to an enzyme-bound topology for the dihydropyridazinone in which the 5-methyl group may assume a pseudoaxial position, orientated approximately orthogonal to the near coplanar core of the two heterocycles. To test this hypothesis we prepared and evaluated a number of torsionally-constrained analogues (Schemes 1 and 2), with coplanarity enforced by introduction of bridging rings from the (dihydro)pyridazinone 5-position to the pyrazolopyridine at either C-2′ or C-4′. In this way we were able to assess the impact of locking the diazine functionality orientated proximal to either the pyrido ring (Scheme 1, Series 1, **13**–**18**) or to the pyrazole ring (Scheme 2, Series 2, **27** and **28**).

Table 1
PDE-inhibitory activity of compounds from Figures 2 and 3 and Schemes 1–3

Compound	Inhibition IC_{50} (μM)		
	PDE3[a]	PDE4[a]	PDE5[a]
Ibudilast	299	5.0	103
KCA-965 (**1**)	89	9.0	44
KCA-1312 (**1R**)	3.8	13	21
KCA-1313 (**1S**)	>400	16	>400
2	110	40	78
3	72	114	79
4	>400	>400	>400
13	7.0	200	145
14	26	11	>400
15	15	30	>400
16	8.9	2.0	>400
17	3.2	73	156
18	69	16	>400
27	210	39	350
28	NI[b]	2.5	>400
29	NI[c]	16	>400
30	260	17	225
31	>400	1.7	>400
32	>400	29	65
33	>400	>400	>400
34	>400	115	>400
41	NI[b]	1.38	NI[b]
42	2.75	2.58	>100
43	41.5	0.055	6.4
44	39.6	2.61	NI[b]
45	33.5	0.12	28.9

[a] Enzyme assays were performed using the core catalytic domains from the PDE3A, PDE4B and PDE5A isoforms according to previously reported protocols.[11b] Data reported are the mean of at least three experiments.[26]
[b] No inhibition up to 100 μM.
[c] No inhibition up to 400 μM.

Compounds **13**–**18** were prepared as summarised in Scheme 1. The known tricycle **9** has been prepared by condensation of 1-aminopyridinium iodide with cyclohexane-1,3-dione.[17] In our hands this reaction was low-yielding (6–12%) and failed altogether for some *N*-aminopyridinium salts substituted at the C-2 position (e.g., 1-amino-2-methoxypyridinium mesitylenesulfonate). We developed an alternative route to **9** using the cycloaddition reaction between alkynoate **6** and pyridine *N*-imine, the latter generated in situ by treatment of 1-aminopyridinium mesitylenesulfonate with K_2CO_3 in DMF. Dieckmann ring closure of cycloadduct **7** afforded tricyclic ketoester **8** which was subsequently hydrolysed with concomitant decarboxylation to give **9**.[18] At this point the route branched in order to access torsionally-constrained analogues of the parent 5-methyldihydropyridazinone (**1**) and the unsubstituted analogue (**2**). Thus, treatment of ketone **9** with base followed by bromoacetate afforded ester **11**. Closure of the dihydropyridazinone ring was accomplished by reaction with hydrazine to give **13**. Dihydropyridazinone **13** was converted into pyridazinone **17** by a standard bromination–dehydrobromination procedure. Insertion of an additional alkylation step into the route (**9** to **10**) prior to the bromoacetate reaction allowed installation of a methyl group at the 5-position of the dihydropyridazinone ring subsequently formed in **15**. The impact of pyridazinone ring N(2)-alkylation was assessed by preparing the *N*-benzyl analogues (**14**, **16** and **18**).

Compounds **27** and **28**, with the pyridazinone ring torsionally-constrained by a tether to the pyrazolopyridine C-4′ centre (Series

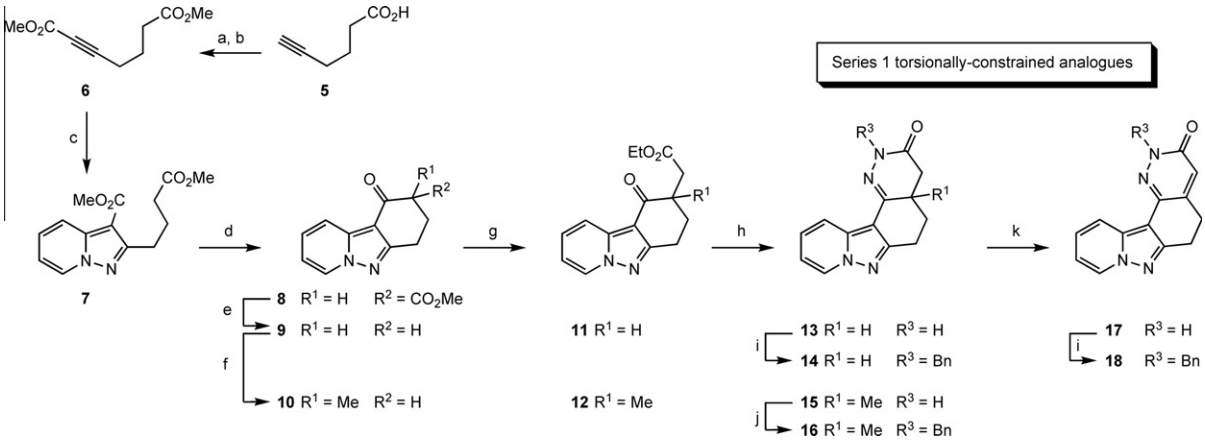

Scheme 1. Reagents and conditions: (a) *n*-BuLi (2.4 equiv), THF, −78 °C, then $ClCO_2Me$; (b) MeOH, HCl (cat.) (68% two steps); (c) 1-aminopyridinium mesitylenesulfonate, K_2CO_3, DMF, 0 °C (49%); (d) LiHMDS, THF, −78 °C, (**8**, 70% from **7**); (e) LiOH, THF, H_2O (**9**, 40% from **8**); (f) LiHMDS, THF, −78 °C, then MeI (**10**, 78% from **9**); (g) LiHMDS, THF, −78 °C, then $BrCH_2CO_2Me$ (**11**, 80% from **9**; **12**, 74% from **10**); (h) $H_2N–NH_2$, AcOH, EtOH, H_2O, reflux (**13**, 80% from **11**; **15**, 51% from **12**); (i) BnBr, Cs_2CO_3, DMF (**14**, 24% from **13**; **18**, 53% from **17**); (j) BnBr, NaH, THF (**16**, 90% from **15**); (k) Br_2, HBr, AcOH, H_2O, reflux (**17**, 92% from **13**).

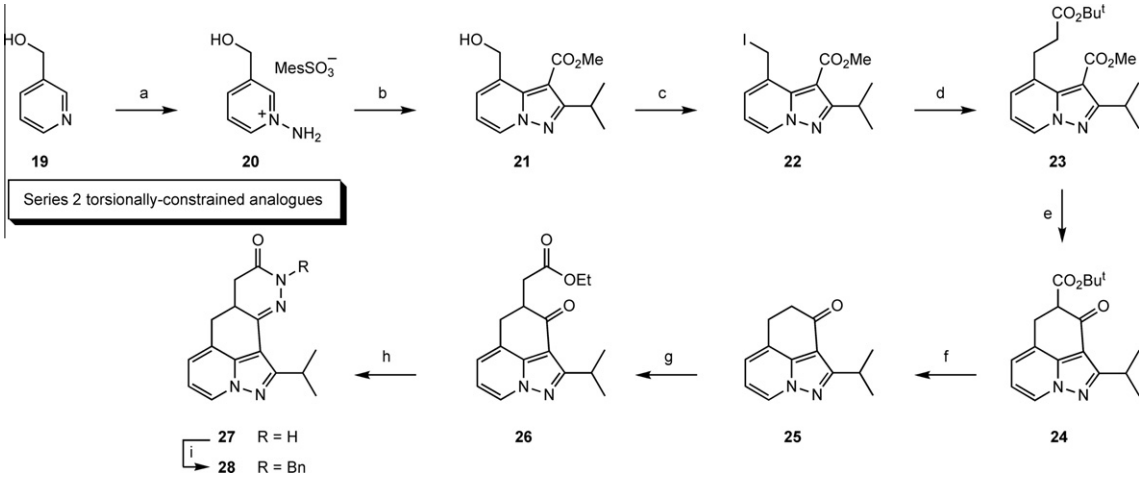

Scheme 2. Reagents and conditions: (a) *O*-mesitylenesulfonyl hydroxylamine, CH_2Cl_2 (62%); (b) methyl 4-methylpent-2-ynoate, K_2CO_3, DMF, 0 °C (66% as 3:2 mixture of 6-hydroxymethyl and 4-hydroxymethyl isomers, the latter (**21**) was separated chromatographically); (c) $MeSO_2Cl$, Et_3N, CH_2Cl_2, then NaI/acetone (80%); (d) $MeCO_2Bu^t$, LiHMDS, THF, −78 °C, then addition of **22** (89%); (e) LiHMDS, THF, −78 °C (93%); (f) CF_3CO_2H, CH_2Cl_2 then PhMe/reflux (74%); (g) LiHMDS, THF, −78 °C, then $BrCH_2CO_2Me$ (57%); (h) $H_2N–NH_2$, AcOH, EtOH, H_2O, reflux (77%); (i) BnBr, NaH, THF (57%).

2), were synthesised via tricyclic ketoester **24**, Scheme 2. The latter was prepared, as shown, by adaptation of a previously reported route to a similar compound starting from pyridine-3-methanol (**19**).[19] The pyridazinone ring in **27** was then constructed in much the same way as for the Series 1 analogues shown in Scheme 1. Thus, cleavage of the ester in **24** with decarboxylation afforded ketone **25**. Reaction of the enolate derived from the latter with bromoacetate led to ketoester **26**. The dihydropyridazinone ring in **27** was completed by reaction with hydrazine. Alkylation of **27** was also applied to afford the *N*-benzyl derivative (**28**).

Activity data for torsionally-constrained analogues **13**–**18**, **27** and **28**, which (for the structures possessing a stereogenic centre) were assessed in racemic form, are summarised in Table 1. PDE5-inhibitory activity was weak in all analogues. The Series 2 parent structure (**27**) exhibited comparable PDE4-inhibitory activity to the unconstrained parent structure (**2**). In contrast, the Series 1 parent structure (**13**) performed less well as a PDE4 inhibitor. The oxidised, Series 1 pyridazinone analogue (**17**) exhibited comparable activity as a PDE4 inhibitor to the corresponding unconstrained structure (**3**). Introduction of the dihydropyridazinone ring 5-methyl group (**15**) and *N*-benzylation of the (dihydro)pyridazinone (**14**, **16**, **18**) markedly improved PDE4-inhibitory potency in Series 1 analogues. However, the *N*-benzyl Series 2 compound (**28**) also exhibited improved performance in the PDE4 assay, suggesting that the unconstrained pyrazolopyridine–pyridazinones may potentially bind the PDE4 catalytic pocket with a near coplanar topology to the ring systems but where the enzyme may tolerate either of the two possible relative orientations for the rings. In contrast to the results with PDE4, the Series 2 torsionally-constrained analogues (**27** and **28**) performed poorly as inhibitors of PDE3, whereas, the Series 1 analogues (**13**, **15**, **17**) showed respectable activity. These data suggest a PDE3-bound conformation in which the pyridazinone ring diazine functionality preferentially lies '*syn*' to the pyrazolopyridine pyrido ring.

In addition to our efforts to probe the enzyme-bound topology of the pyrazolopyridine–pyridazinone inhibitors, we also undertook a SAR survey, focusing mainly on pyridine ring substitutions and modifications to the pyridazinone ring lactam functionality. The most important findings from this work are concisely summarised with reference to the compounds shown in Figure 3, which were prepared using the synthetic routes recently described by us.[16] Substitutions at the N(2)- and 7′-positions were found to offer

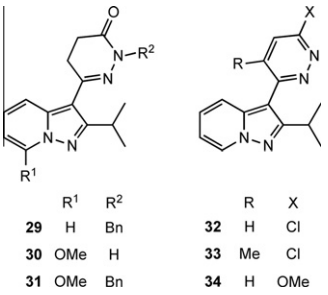

	R^1	R^2		R	X
29	H	Bn	**32**	H	Cl
30	OMe	H	**33**	Me	Cl
31	OMe	Bn	**34**	H	OMe

Figure 3. Representative 6-(pyrazolo[1,5-*a*]pyridin-3-yl)pyridazin-3(2*H*)-ones and related compounds that provided informative SAR data.

greatest potential for enhancement of PDE4 inhibitory activity, and a combination of 7′-methoxy with N(2)-benzyl (**29**–**31**) was particularly effective (Table 1). The enhancement of PDE4-inhibitory activity achieved with *N*-benzylation (**29** and **31**) mirrors the effect seen in the *N*-benzyl torsionally-constrained analogues (**14**, **16**, **18**, **28**) when compared with their respective parent structures (**13**, **15**, **17**, **27**). For PDE3 inhibition *N*-benzylation reduced activity in the torsionally-constrained series (with the exception of compound **16**, where a slight improvement of activity was seen over parent **15**). In the unconstrained compounds (**29** and **31**) the reduction in PDE3-inhibitory activity with *N*-benzylation was more pronounced. This effect was also reproduced with a range of substituents (data not shown), and N(2)-alkylation consistently compromised inhibition of PDE3 (and PDE5) but enhanced inhibition of PDE4. Chlorination of the pyridazinone ring (**32**) or transformation to the methoxypyridazine (**34**) also caused a collapse in PDE3 inhibition whilst allowing retention or improvement in the modest PDE4-inhibitory activity of parent **3**. The presence of the in-plane 5-methyl group in pyridazine **33** caused loss of activity across the panel, mirroring the effect seen with pyridazinone **4**. The key finding here was that PDE3-inhibitory activity in the pyrazolopyridine–pyridazinone series is critically dependent on the lactam functionality of the (dihydro)pyridazinone ring. This is consistent with a binding mode in which the pyridazinone engages the purine-scanning Gln and distal His of the catalytic pocket, as seen in the X-ray co-crystal structure of the PDE3B core catalytic domain in complex with another 5-methyldihydropyridazinone-containing ligand.[20] Such a binding mode accounts for the topological preferences for inhibitor binding to PDE3 deduced from our torsionally-constrained series. Thus, only the Series 1 structures can fit the PDE3 catalytic pocket in this mode, as shown for compound **15** (*S*-ent) docked into the PDE3B structure, Figure 4A. Significantly, this binding mode also accounts for the stereochemical discrimination between **1R** and **1S** exhibited by PDE3. Thus, a 5-methyl group occupying the pseudoaxial position, and orientated approximately orthogonal to the near coplanar core heterocycle arrangement, can only be accommodated on one face of the ligand. In the case of **1R** and **15** (*S*-ent) the methyl group is predicted to fit a small subpocket adjacent to the purine-stacking Phe residue. The methyl group of **1S** and **15** (*R*-ent) cannot be accommodated in such a binding mode, thus the activity of **15** is predicted to reside with the (*S*)-enantiomer, although we did not confirm this by separate evaluation of the two enantiomers for **15**.

In PDE4 Tyr takes the place of the distal His of PDE3 and the conformational preferences of the purine-scanning Gln differ somewhat between PDE3 and PDE4, thereby contributing to the cAMP-binding specificity exhibited by PDE4 isoforms.[22] The retention of PDE4-inhibitory activity in chloropyridazine **32** as well as the insensitivity of PDE4 to the stereochemistry of **1R**/**1S** and the activity enhancement associated with introduction of the 7′-methoxy group (**30** and **31**) are all indicative of a ligand binding mode in PDE4 which is fundamentally different from that which operates for PDE3. Hydrogen-bonded engagement of the purine-scanning glutamine is a universal feature seen in co-crystal structures of inhibitors bound to PDE4, and the SAR data presented here suggest that it is the pyrazolopyridine subunit (not the pyridazinone) that fulfils this role in our compound series. This implies that the compounds bind in reverse orientation in PDE4 (relative to PDE3), such that the pyridazinone ring occupies the region proximal to the catalytic metal centres in PDE4. The binding mode for **30** and **31** would then be reminiscent of that established for catechol ether PDE4 inhibitors such as zadaverine[21,23] and roflumilast,[21,24] with the pyrazolopyridine N(1′) and 7′-OMe groups hydrogen bonding to the purine-scanning Gln (Fig. 4B).

Consideration of the PDE4 binding model for compounds such as **30** (Fig. 4B) suggested that interaction of the (dihydro)pyridazinone ring within the catalytic pocket may be suboptimal. This led us to investigate the impact of repositioning its site of attachment from C-3′ to C-4′ of the pyrazolopyridine in order to set the ring more deeply within the catalytic pocket and improve surface contact with the protein. We therefore prepared a test set of '4′-linked' analogues (**41–45**) for evaluation, Scheme 3. The synthetic strategy employed a Suzuki coupling of 3,6-dichloropyridazine with a pyrazolopyridine-4-boronic acid derived from bromide **39**,

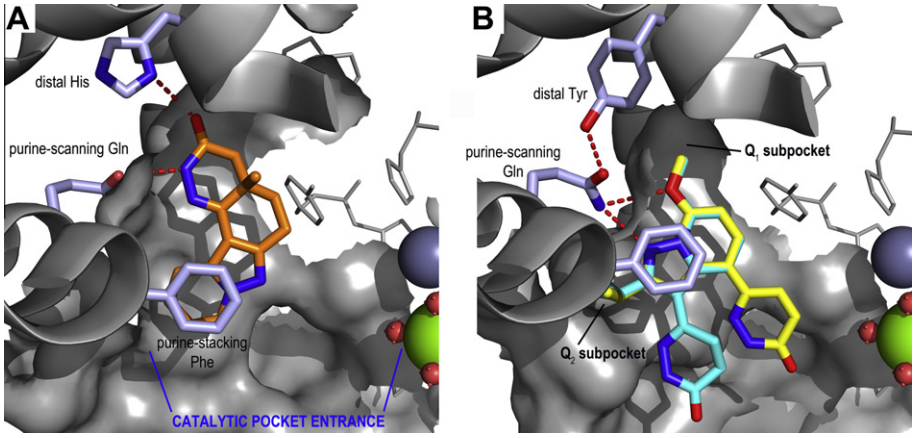

Figure 4. (A) Model of **15** (*S*-ent) (orange stick) docked into the catalytic pocket of PDE3B (PDB: 1SO2[20]). An alternative binding mode in which the inhibitor oxygen hydrogen bonds to the purine-scannning Gln (rather than the distal His) may operate for some compounds alkylated on the pyridazinone N(2) (e.g., **14**, **16**). (B) Models of **30** (cyan stick) and **42** (yellow stick) docked into the catalytic pocket of PDE4D (PDB: 1XOR[21]). Hydrophobic pyridazinone N(2)-substituents (e.g., Bn in **43**, **45**) favourably extend surface contact with residues around the catalytic pocket rim.

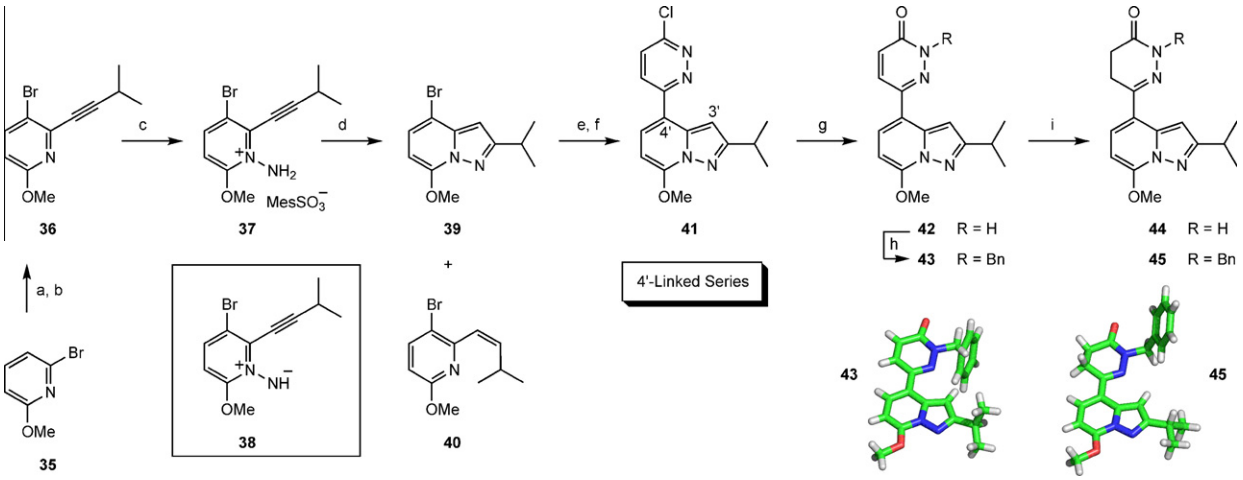

Scheme 3. Reagents and conditions: (a) NBS, MeCN, 90 °C (53%); (b) 3-methyl-1-butyne, $Pd(TPP)_4$, CuI, THF, Pr^i_2NH, 70 °C (sealed tube) (97%); (c) *O*-mesitylenesulfonyl hydroxylamine, CH_2Cl_2, (d) K_2CO_3, DMF (**39**, 28% two steps from **37**); (e) (1) *n*-BuLi, THF, −78 °C, (2) $B(OMe)_3$, −78 °C to 20 °C, (3) SiO_2 chromatography (34%); (f) 3,6-dichloropyridazine, $Pd(PPh_3)_4$, Na_2CO_3 (aq), THF, reflux (72%); (g) AcOH, reflux (**42**, 59% from **41**); (h) BnBr, NaH, THF; (i) Zn, AcOH, 110 °C, 10 min (**44**, 35% from **42**; **45**, 83% from **43**). [X-ray crystal structures of **43** and **45** are shown.][30]

the latter prepared from pyridine **35**. Thus, bromination of **35** with NBS in hot MeCN afforded 2,3-dibromo-6-methoxypyridine in 53% isolated yield after an easy separation from the minor 2,5-dibromide product by crystallization. Sonogashira coupling with 3-methyl-1-butyne efficiently produced alkynylpyridine **36**. Amination of **36** with *O*-mesitylenesulfonyl hydroxylamine followed by cyclisation of the resulting *N*-aminopyridinium salt (**37**) under basic conditions via the pyridine *N*-imine (**38**) produced bicycle **39** in 28% yield. Simple 1-amino-2-(alk-1-ynyl)pyridinium salts undergo reasonably efficient cyclisation to pyrazolo[1,5-*a*]pyridines.[25] In the reaction leading to **39**, however, competing deamination of *N*-aminopyridinium salt **37** and intermediate pyridine *N*-imine **38** was observed, which returned alkynylpyridine **36** together with the reduced alkenylpyridine derivative (**40**). Copious quantities of N_2 gas were generated during the base treatment of the salt **37** and this suggests a decomposition mechanism in which the pyridine *N*-imine deaminates the salt to generate diimine. The production of diimine then accounts for both the reduction of the alkyne side chain, affording the *cis*-alkene (**40**), and for the observed evolution of N_2. Pyrazolopyridine **39** was boronated under standard conditions by lithium–bromine exchange followed by reaction with trimethylborate. The intermediate boronic acid was then used in the Suzuki coupling with 3,6-dichloropyridazine to afford **41**. Solvolysis of **41** with hot acetic acid gave pyridazinone **42** and thence dihydropyridazinone **44** after reduction with zinc dust in acetic acid. Pyridazinone **42** was also *N*-benzylated to give **43**, which was subsequently reduced to **45**.

Pleasingly, activity data for **41**–**45** confirmed out hypothesis that repositioning of the (dihydro)pyridazinone would enhance PDE4-inhibitory potency. Thus, compounds **44** and **45** exhibited 6.5- and 14-fold enhancements of PDE4-inhibitory activity over their isomeric 3′-linked counterparts (**30** and **31**, respectively). The improvement in PDE4 inhibition was particularly striking with *N*-benzylpyridazinone **43** (IC_{50} 55 nM). Significantly, pyridazinone **42** and chloropyridazine **41** possessed comparable activity as PDE4 inhibitors, consistent with the proposed PDE4 binding mode (Fig. 4B) in which the pyridazinone does not contribute key hydrogen bond sites. In contrast, the low micromolar PDE3-inhibitory activity of **42** was completely lost in chloropyridazine **41**. As with the 3′-linked pyrazolopyridine–pyridazinones, this suggests that the preferred binding mode for 4′-linked compounds involves the pyridazinone ring in hydrogen bonded engagement of residues in the distal region of the PDE3 catalytic pocket. The near coplanar enzyme-bound core structure arrangement of the inhibitors is likely to be preserved in the 4′-linked compound series, and indeed this conformation is also observed in the solid state single crystal X-ray structures of the two most potent PDE4-inhibitory compounds in the series (**43** and **45**), Scheme 3.

The results presented here suggest that the nonselective PDE-inhibitory activity of ibudilast likely arises from the capacity of this small structure to fit the catalytic pockets of all the PDE families, with a hydrogen bond established from the pyrazolopyridine N(1) centre to the conserved purine-scanning glutamine residue of these enzymes. The structural modifications that we have described establish a firm basis for development of both potent PDE4-selective and dual PDE3/4-selective inhibitors derived from ibudilast. Compound **42**, in particular, possesses well-balanced PDE3- and PDE4-inhibitory activity with considerable selectivity over PDE5. In contrast, *N*-benzyl pyridazinone **43** exhibits potent activity against PDE4 with 2–3 magnitude orders of selectivity over PDE5 and PDE3.

Acknowledgments

PyMOL from W.L. DeLano, DeLano Scientific, was used to create the protein structure images in this work. We thank the EPSRC Mass Spectrometry Centre at Swansea for mass spectra and Dr S.J. MacKenzie, Dr S. Hastings and Dr R.A. Clayton of the Kyorin Scotland Research Laboratory for performing PDE inhibition assays.

References and notes

1. Giovannoni, M. P.; Vergelli, C.; Graziano, A.; Dal Piaz, V. *Curr. Med. Chem.* **2010**, *17*, 2564.
2. Klocke, R. K.; Mager, G.; Kux, A.; Hopp, H. W.; Hilger, H. H. *Am. Heart J.* **1991**, *121*, 1965.
3. (a) Packer, M.; Carver, J. R.; Rodeheffer, R. J.; Ivanhoe, R. J.; DiBianco, R.; Zeldis, S. M.; Hendrix, G. H.; Bommer, W. J.; Elkayam, U.; Kukin, M. L., et al *N. Engl. J. Med.* **1991**, *325*, 1468; (b) Nony, P.; Boissel, J. P.; Lievre, M.; Leizorovicz, A.; Haugh, M. C.; Fareh, S.; de Breyne, B. *Eur. J. Clin. Pharmacol.* **1994**, *46*, 191.
4. (a) Thompson, P. E.; Manganiello, V.; Degerman, E. *Curr. Top. Med. Chem.* **2007**, *7*, 421; (b) Movsesian, M.; Stehlik, J.; Vandeput, F.; Bristow, M. R. *Heart Fail. Rev.* **2009**, *14*, 255.
5. (a) Teixeira, M. M.; Gristwood, R. W.; Cooper, N.; Hellewell, P. G. *Trends Pharmacol. Sci.* **1997**, *18*, 164; (b) Doherty, A. M. *Curr. Opin. Chem. Biol.* **1999**, *3*, 466; (c) Houslay, M. D.; Schafer, P.; Zhang, K. Y. *Drug Discovery Today* **2005**, *10*, 1503; (d) Huang, Z.; Mancini, J. A. *Curr. Med. Chem.* **2006**, *13*, 3253; (e) Dastidar, S. G.; Rajagopal, D.; Ray, A. *Curr. Opin. Investig. Drugs* **2007**, *8*, 364.

6. (a) Rose, G. M.; Hopper, A.; De Vivo, M.; Tehim, A. *Curr. Pharm. Des.* **2005**, *11*, 3329; (b) Reneerkens, O. A.; Rutten, K.; Steinbusch, H. W.; Blokland, A.; Prickaerts, J. *Psychopharmacology (Berl.)* **2009**, *202*, 419.
7. Giembycz, M. A.; Field, S. K. *Drug Des. Develop. Ther.* **2010**, *4*, 147.
8. Chung, K. F. *Eur. J. Pharmacol.* **2006**, *533*, 110.
9. Torphy, T. J.; Undem, B. J.; Cieslinski, L. B.; Luttmann, M. A.; Reeves, M. L.; Hay, D. W. *J. Pharmacol. Exp. Ther.* **1993**, *265*, 1213.
10. (a) Van der Mey, M.; Bommele, K. M.; Boss, H.; Hatzelmann, A.; Van Slingerland, M.; Sterk, G. J.; Timmerman, H. *J. Med. Chem.* **2003**, *46*, 2008; (b) Giembycz, M. A. *Proc. Am. Thorac. Soc.* **2005**, *2*, 326; (c) Boswell-Smith, V.; Spina, D.; Oxford, A. W.; Comer, M. B.; Seeds, E. A.; Page, C. P. *J. Pharmacol. Exp. Ther.* **2006**, *318*, 840; (d) Banner, K. H.; Press, N. J. *Br. J. Pharmacol.* **2009**, *157*, 892; (e) Yamazaki, T.; Anraku, T.; Matsuzawa, S. *Eur. J. Pharmacol.* **2011**, *650*, 605.
11. (a) Kishi, Y.; Ohta, S.; Kasuya, N.; Sakita, S.; Ashikaga, T.; Isobe, M. *Cardiovasc. Drug Rev.* **2001**, *19*, 215; (b) Gibson, L. C. D.; Hastings, S. F.; McPhee, I.; Clayton, R. A.; Darroch, C. E.; Mackenzie, A.; MacKenzie, F. L.; Nagasawa, M.; Stevens, P. A.; MacKenzie, S. J. *Eur. J. Pharmacol.* **2006**, *538*, 39; (c) Huang, Z.; Liu, S.; Zhang, L.; Salem, M.; Greig, G. M.; Chan, C. C.; Natsumeda, Y.; Noguchi, K. *Life Sci.* **2006**, *78*, 2663.
12. (a) Kohno, Y.; Ogata, T.; Awano, K.; Matsuzawa, K.; Tooru, T. PCT Int. Appl. Patent WO9814448, 1998.; (b) Yoshida, N.; Aono, M.; Tsubuki, T.; Awano, K.; Kobayashi, T. *Tetrahedron: Asymmetry* **2003**, *14*, 529; (c) Yoshida, N.; Awano, K.; Kobayashi, T.; Fujimori, K. *Synthesis* **2004**, 1554.
13. Sircar, I.; Duell, B. L.; Bobowski, G.; Bristol, J. A.; Evans, D. B. *J. Med. Chem.* **1985**, *28*, 1405.
14. Bristol, J. A.; Sircar, I.; Moos, W. H.; Evans, D. B.; Weishaar, R. E. *J. Med. Chem.* **1984**, *27*, 1099.
15. Schudt, C.; Winder, S.; Muller, B.; Ukena, D. *Biochem. Pharmacol.* **1991**, *42*, 153.
16. Johnston, K. A.; Allcock, R. W.; Jiang, Z.; Collier, I. D.; Blakli, H.; Rosair, G. M.; Bailey, P. D.; Morgan, K. M.; Kohno, Y.; Adams, D. R. *Org. Biomol. Chem.* **2008**, *6*, 175.
17. Tamura, Y.; Tsujimoto, N.; Sumida, Y.; Ikeda, M. *Tetrahedron* **1972**, *28*, 21.
18. This route to the tricyclic ketone was more versatile as it could be successfully applied with other *N*-aminopyridinium salts such as the 2-methoxy substituted salt (not shown).
19. (a) Gmeiner, P.; Sommer, J. *Arch. Pharm. (Weinheim, Ger.)* **1994**, *327*, 435; (b) Gmeiner, P.; Sommer, J.; Mierau, J.; Höfner, G. *Bioorg. Med. Chem. Lett.* **1993**, *3*, 1477.
20. Scapin, G.; Patel, S. B.; Chung, C.; Varnerin, J. P.; Edmondson, S. D.; Mastracchio, A.; Parmee, E. R.; Singh, S. B.; Becker, J. W.; Van der Ploeg, L. H.; Tota, M. R. *Biochemistry* **2004**, *43*, 6091.
21. Card, G. L.; England, B. P.; Suzuki, Y.; Fong, D.; Powell, B.; Lee, B.; Luu, C.; Tabrizizad, M.; Gillette, S.; Ibrahim, P. N.; Artis, D. R.; Bollag, G.; Milburn, M. V.; Kim, S. H.; Schlessinger, J.; Zhang, K. Y. J. *Structure* **2004**, *12*, 2233.
22. (a) Houslay, M. D.; Adams, D. R. *Biochem. J.* **2003**, *370*, 1; (b) Zhang, K. Y. J.; Card, G. L.; Suzuki, Y.; Artis, D. R.; Fong, D.; Gillette, S.; Hsieh, D.; Neiman, J.; West, B. L.; Zhang, C.; Milburn, M. V.; Kim, S. H.; Schlessinger, J.; Bollag, G. *Mol. Cell* **2004**, *15*, 279; (c) Ke, H.; Wang, H. *Curr. Top. Med. Chem.* **2007**, *7*, 391; (d) Wang, H.; Robinson, H.; Ke, H. *J. Mol. Biol.* **2007**, *371*, 302.
23. Lee, M. E.; Markowitz, J.; Lee, J. O.; Lee, H. *FEBS Lett.* **2002**, *530*, 53.
24. Burgin, A. B.; Magnusson, O. T.; Singh, J.; Witte, P.; Staker, B. L.; Bjornsson, J. M.; Thorsteinsdottir, M.; Hrafnsdottir, S.; Hagen, T.; Kiselyov, A. S.; Stewart, L. J.; Gurney, M. E. *Nat. Biotechnol.* **2010**, *28*, 63.
25. (a) Tsuchuja, T.; Sashida, H.; Konoshita, A. *Chem. Pharm. Bull.* **1983**, *31*, 4568; (b) Tsuchuja, T.; Sashida, H. *J. Chem. Soc., Chem. Commun.* **1980**, 1109.
26. The isolated catalytic domains of PDE3A, PDE4B and PDE5A were used in our primary assays and the inhibitory potencies found for ibudilast differ from those reported in earlier studies,[11b,c] which used different constructs. We evaluated compound activity against the PDE core catalytic domains in our foundational studies because sensitivity to inhibitors can be influenced by the nature of the N-terminal regulatory regions, especially for the PDE4 enzymes. These are encoded by four genes (*PDE4A–D*) that each give rise to multiple isoforms.[22a,27] The isoforms are categorised as 'long', 'short' or 'supershort' according to the presence or absence of regulatory modules, upstream conserved regions 1 and 2 (UCR1, UCR2), located between a unique isoform-specific N-terminal sequence and the core catalytic domain.[22a] The UCR modules transduce the functional consequences of regulatory phosphorylation by kinases such as PKA,[22a] but we have recently shown that ibdudilast is one of a group of inhibitors that can interact with a 'gating sequence' in UCR2, switching the PDE4 conformational state to one in which the inhibitor-occupied catalytic pocket is capped by UCR2.[28] Such conformational switching can lead to profound changes in inhibitor affinities and is sensitive to both phosphorylation and partner protein binding.[29] Thus, for the archetypal PDE4 inhibitor, rolipram, conformational interchange can switch PDE4 enzymes between low-affinity and high-affinity rolipram binding states (LARBS/HARBS) with IC_{50}s in the micromolar and nanomolar ranges, respectively.[22a]
27. Conti, M.; Richter, W.; Mehats, C.; Livera, G.; Park, J. Y.; Jin, C. *J. Biol. Chem.* **2003**, *278*, 5493.
28. (a) Terry, R.; Cheung, Y. F.; Praestegaard, M.; Baillie, G. S.; Huston, E.; Gall, I.; Adams, D. R.; Houslay, M. D. *Cell. Signal.* **2003**, *15*, 955; (b) Christian, F.; Anthony, D. F.; Vadrevu, S.; Riddell, T.; Day, J. P.; McLeod, R.; Adams, D. R.; Baillie, G. S.; Houslay, M. D. *Cell. Signal.* **2010**, *22*, 1576; (c) Day, J. P.; Lindsay, B.; Riddell, T.; Jiang, Z.; Allcock, R. W.; Abraham, A.; Sookup, S.; Christian, F.; Bogum, J.; Martin, E. K.; Rae, R. L.; Anthony, D.; Rosair, G. M.; Houslay, D. M.; Huston, E.; Baillie, G. S.; Klussmann, E.; Houslay, M. D.; Adams, D. R. *J. Med. Chem.* **2011**, doi:10.1021/jm200070e.
29. (a) Houslay, M. D.; Adams, D. R. *Nat. Biotechnol.* **2010**, *28*, 38; (b) Alvarez, R.; Sette, C.; Yang, D.; Eglen, R. M.; Wilhelm, R.; Shelton, E. R.; Conti, M. *Mol. Pharmacol.* **1995**, *48*, 616; (c) McPhee, I.; Yarwood, S. J.; Scotland, G.; Huston, E.; Beard, M. B.; Ross, A. H.; Houslay, E. S.; Houslay, M. D. *J. Biol. Chem.* **1999**, *274*, 11796; (d) Saldou, N.; Obernolte, R.; Huber, A.; Baecker, P. A.; Wilhelm, R.; Alvarez, R.; Li, B.; Xia, L.; Callan, O.; Su, C.; Jarnagin, K.; Shelton, E. R. *Cell. Signal.* **1998**, *10*, 427.
30. The X-ray CIF files for **43** and **45** have been deposited at the Cambridge Crystallographic Data Center with the deposition numbers CCDC 811960 and CCDC 811961. Copies of the data can be obtained, free of charge, from CCDC, 12 Union Road, Cambridge, CB2 1EZ UK (e-mail: deposit@ccdc.cam.ac.uk; Internet: //www.ccdc.cam.ac.uk).